THE JOURNAL OF PHYSICAL CHEMISTRY B

Article

pubs.acs.org/JPCB

Toward an Accurate Modeling of Hydrodynamic Effects on the Translational and Rotational Dynamics of Biomolecules in Many-Body Systems

Maciej Długosz*,† and Jan M. Antosiewicz‡

†Centre of New Technologies, University of Warsaw, Stefana Banacha 2c, Warsaw 02-097, Poland

‡Department of Biophysics, Faculty of Physics, University of Warsaw, Zwirki i Wigury 93, Warsaw 02-089, Poland

Supporting Information

ABSTRACT: Proper treatment of hydrodynamic interactions is of importance in evaluation of rigid-body mobility tensors of biomolecules in Stokes flow and in simulations of their folding and solution conformation, as well as in simulations of the translational and rotational dynamics of either flexible or rigid molecules in biological systems at low Reynolds numbers. With macromolecules conveniently modeled in calculations or in dynamic simulations as ensembles of spherical frictional elements, various approximations to hydrodynamic interactions, such as the two-body, far-field Rotne−Prager approach, are commonly used, either without concern or as a compromise between the accuracy and the numerical complexity. Strikingly, even though the analytical Rotne−Prager approach fails to describe (both in the qualitative and quantitative sense) mobilities in the simplest system consisting of two spheres, when the distance between their surfaces is of the order of their size, it is commonly applied to model hydrodynamic effects in macromolecular systems. Here, we closely investigate hydrodynamic effects in two and three-body systems, consisting of bead−shell molecular models, using either the analytical Rotne−Prager approach, or an accurate numerical scheme that correctly accounts for the many-body character of hydrodynamic interactions and their short-range behavior. We analyze mobilities, and translational and rotational velocities of bodies resulting from direct forces acting on them. We show, that with the sufficient number of frictional elements in hydrodynamic models of interacting bodies, the far-field approximation is able to provide a description of hydrodynamic effects that is in a reasonable qualitative as well as quantitative agreement with the description resulting from the application of the virtually exact numerical scheme, even for small separations between bodies.

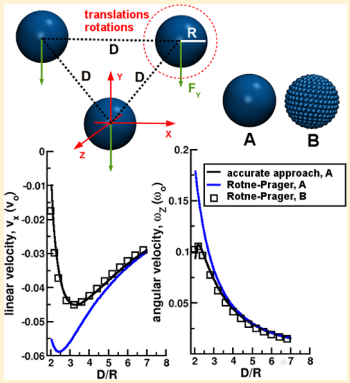

INTRODUCTION

Molecules translating and rotating in a viscous fluid generate a flow field that couples their motions. This coupling is the origin of so-called hydrodynamic interactions (HI). While the general role of HI in modulating the dynamic properties of biological systems is widely recognized, and their possible effects on protein−protein or protein−ligand association,[1−5] protein folding and unfolding,[6−8] formation of lipid bilayers,[9] and diffusional transport in cytosol-like environments[10,11] have been theoretically investigated using particle-based simulation techniques, the main problem of such studies still remains the proper account of HI in complex systems consisting of biomolecules with diverse sizes and shapes. This is due to the fact, that HI have many-body character and depend in a complicated, nonlinear fashion on positions and orientations of all molecules in the considered system.

In a system of spheres, which is usually an appropriate description of colloids, HI can, in principle, be modeled accurately in computer simulations, employing for example techniques of Stokesian[12] or Brownian dynamics,[13] using expressions for mobility tensors in the form of power series of the inverse of interparticle distances.[11,14−16]

While biological molecules are rarely spherical, their complicated shapes can be accounted for by representing them as conglomerates of spherical frictional elements which, depending on the purpose, can be either internally flexible[1,7,8] or rigid.[5,17−23] Thus, their mobility tensors and HI can, at least in theory, be evaluated accurately using hydrodynamic approaches from the field of colloids. However, the numerical complexity as well as the high computational cost of such an accurate HI treatment are reasons why, in calculations and dynamic simulations of biomolecules, various approximations are usually employed. As far as biological systems are considered, the Rotne−Prager (RP) tensor[24] (and its extensions[25−27]) is probably the most popular of such approximations.[1−3,6−9,20−23,28−31] It has been employed for example to investigate folding and mechanical properties of flexible, coarse-grained models of proteins,[6−8] facilitated diffusion of proteins on DNA with DNA modeled as flexible bead chains,[29,30] association of proteins,[1] formation of lipid membranes,[9] and diffusion of spherical proteins near charged surfaces.[31] It has also been a basis for rigid-body

Received: May 16, 2015
Published: June 11, 2015

DOI: 10.1021/acs.jpcb.5b04675
J. Phys. Chem. B 2015, 119, 8425−8439

hydrodynamic calculations of mobility tensors of arbitrarily shaped biomolecules represented with models consisting of spherical frictional elements.[19−23]

The popularity of the Rotne−Prager approach in modeling of, often quite complex, biological systems is perhaps somewhat surprising if one considers its far-field, two-body character.[24,26] Strictly speaking, applications of the RP tensor should be limited to systems consisting of well-separated objects. Notably, even when applied to a two-sphere system, the Rotne−Prager approach fails to correctly describe its dynamics when the distance between surfaces of spheres is comparable to their size (this is illustrated below). In practice, however, the RP approximation is used to model biological systems consisting of closely packed spherical frictional elements that constitute for instance flexible, coarse-grained models of polymers and proteins or rigid models of macromolecules.[1−3,6−9,20−23,28−31]

In the current work we investigate the performance of the Rotne−Prager approximation applied to model hydrodynamic effects on the translational and rotational dynamics in two and three-body systems, consisting of conglomerates of spherical frictional elements. As a reference, we use a virtually exact numerical scheme for evaluating HI, the induced forces method proposed in ref 15. We analyze and compare mobility tensors and translational and rotational velocities of bodies, resulting from net direct forces and torques, in the considered systems, calculated using these two approaches. We show, that when the number of frictional elements used to construct hydrodynamic models of interacting bodies is sufficiently large, the RP approximation is able to provide a description of hydrodynamic effects, even for nearly touching bodies, that is in a reasonable qualitative and quantitative agreement with the description resulting from the application of the sophisticated numerical scheme accounting for many-body character and short-range behavior of HI.

METHODS

Hydrodynamic Interactions. Considering a system of N spherical particles suspended in an unbounded viscous fluid at low Reynolds number (so that the creeping flow equations are applicable), we may write the following equations that relate the translational ($\vec{v}_i$) and rotational ($\vec{\omega}_i$) velocities of the particles to the net direct (resulting either from interactions with external fields or interactions with other suspended particles) forces ($\vec{F}_i$) and torques ($\vec{T}_i$) that act on the particles:

$$\vec{v}_i = \sum_{j=1}^{N} (\mu_{ij}^{tt}\vec{F}_j + \mu_{ij}^{tr}\vec{T}_j) \tag{1}$$

$$\vec{\omega}_i = \sum_{j=1}^{N} (\mu_{ij}^{rt}\vec{F}_j + \mu_{ij}^{rr}\vec{T}_j) \tag{2}$$

where i runs over all particles. Coupling of translations (tt) and rotations (rr) of the particles is introduced in the above equations through mobility tensors of rank 2, denoted as μ_{ij}^{tt}, μ_{ij}^{rr}, μ_{ij}^{tr}, and μ_{ij}^{rt}. These tensors are functions of coordinates of all objects in the system. Equations 1 and 2 can be written more compactly if we introduce vectors of generalized velocities $\vec{V} = (\vec{v}_1, ..., \vec{v}_N, \vec{\omega}_1, ..., \vec{\omega}_N)$ and forces $\vec{f} = (\vec{F}_1, ..., \vec{F}_N, \vec{T}_1, ..., \vec{T}_N)$:

$$\vec{V} = \mathbf{M}\vec{f} \tag{3}$$

where $\boldsymbol{M}$ denotes the $6N \times 6N$ generalized mobility matrix:

$$\mathbf{M} = \begin{pmatrix} \mu_{11}^{tt} & \cdots & \mu_{1N}^{tt} & \mu_{11}^{tr} & \cdots & \mu_{1N}^{tr} \\ \cdots & \cdots & \cdots & \cdots & \cdots & \cdots \\ \mu_{N1}^{tt} & \cdots & \mu_{NN}^{tt} & \mu_{N1}^{tr} & \cdots & \mu_{NN}^{tr} \\ \mu_{11}^{rt} & \cdots & \mu_{1N}^{rt} & \mu_{11}^{rr} & \cdots & \mu_{1N}^{rr} \\ \cdots & \cdots & \cdots & \cdots & \cdots & \cdots \\ \mu_{N1}^{rt} & \cdots & \mu_{NN}^{rt} & \mu_{N1}^{rr} & \cdots & \mu_{NN}^{rr} \end{pmatrix} \tag{4}$$

Thus, for a given configuration of the considered system, in order to calculate velocities resulting from forces and torques acting on the particles, (which is usually required in different simulation schemes,[13,32−34]) one needs to evaluate their mobilities.

Tensors $\mu^{\alpha\beta}{}_{ij}$ that constitute $\boldsymbol{M}$ (eq 4) can be conveniently evaluated, using the Rotne−Prager approximation, according to which:[24,26]

$$\mu_{ii}^{tt} = \mu^{t}\mathbf{1} \tag{5}$$

$$\mu_{ij}^{tt} = \mu^{t}\left(\frac{3}{4}\frac{\sigma}{r_{ij}}(\mathbf{1} + \hat{r}_{ij}\hat{r}_{ij}) + \frac{1}{2}\left(\frac{\sigma}{r_{ij}}\right)^3(\mathbf{1} - 3\hat{r}_{ij}\hat{r}_{ij})\right) \tag{6}$$

$$\mu_{ii}^{rr} = \mu^{r}\mathbf{1} \tag{7}$$

$$\mu_{ij}^{rr} = -\mu^{r}\frac{1}{2}\left(\frac{\sigma}{r_{ij}}\right)^3(\mathbf{1} - 3\hat{r}_{ij}\hat{r}_{ij}) \tag{8}$$

$$\mu_{ii}^{tr} = \mathbf{0} \tag{9}$$

$$\mu_{ij}^{tr} = \mu^{r}\sigma\left(\frac{\sigma}{r_{ij}}\right)^2\hat{r}_{ij}\times \tag{10}$$

$$\mu_{ij}^{rt} = (\mu_{ji}^{tr})^{T} \tag{11}$$

where σ is the radius (assumed to be the same for all particles in the system), $r = |\vec{r}|$, $\hat{r} = (\vec{r})/(r)$, dyadic product $\hat{r}\,\hat{r}$ projects onto direction $\hat{r}$, $\hat{r}_{ij}\times$ is a skew-symmetric matrix:

$$\hat{r}_{ij}\times = \begin{pmatrix} 0 & -\left(\frac{z_i - z_j}{r_{ij}}\right) & \frac{y_i - y_j}{r_{ij}} \\ \frac{z_i - z_j}{r_{ij}} & 0 & -\left(\frac{x_i - x_j}{r_{ij}}\right) \\ -\left(\frac{y_i - y_j}{r_{ij}}\right) & \frac{x_i - x_j}{r_{ij}} & 0 \end{pmatrix} \tag{12}$$

and

$$\mu^{t} = \frac{1}{6\pi\eta\sigma} \tag{13}$$

$$\mu^{r} = \frac{1}{8\pi\eta\sigma^3} \tag{14}$$

are translational (t) and rotational (r) self-mobilities of an isolated sphere of a hydrodynamic radius σ, suspended in a fluid

DOI: 10.1021/acs.jpcb.5b04675
J. Phys. Chem. B 2015, 119, 8425−8439

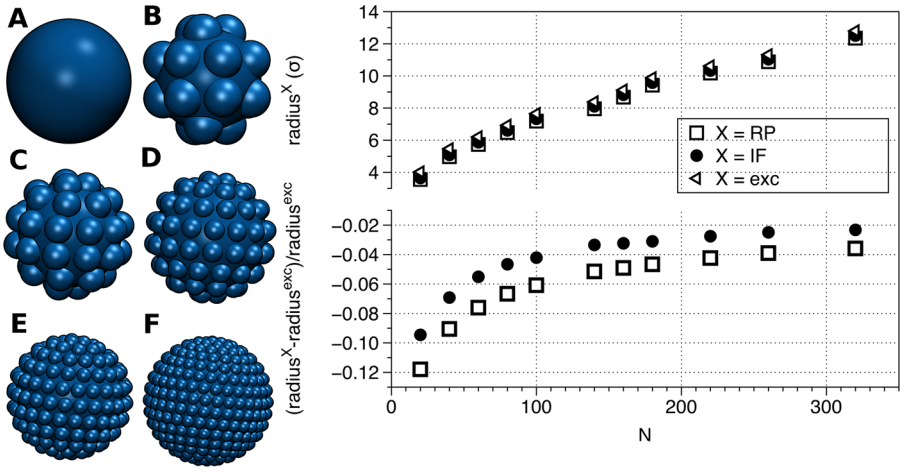

Figure 1. Left: examples of spherical bodies considered in the present study that consist of (A) a single sphere or (B) 20 spherical subunits, (C) 40 spherical subunits, (D) 80 spherical subunits, (E) 160 spherical subunits, or (F) 320 spherical subunits, equidistributed on a surface of a sphere (see text for details). Drawings were done with the VMD package.[40] Right: excluded volume radii (exc) of models from the left panel and their hydrodynamic radii resulting from calculations utilizing the Rotne–Prager approximation (RP) and the induced forces approach (IF). N denotes the number of spheres in a rigid conglomerate. σ is the value of the excluded volume radius as well as the hydrodynamic radius of a single sphere (left panel, A). σ is also the radius of spherical subunits building conglomerates shown in the left panel (B–F) (models A–F in the left panel are not shown to scale).

Table 1. Comparison of Translational (TT) and Rotational (RR) Self-Mobilities of Bead–Shell Models (See Figure 1) Considered in the Current Work, Calculated Using either the Rotne–Prager Approximation (RP) or the Induced Forces Method (IF)[a]

N	$(((\mu^{TT,RP})/(\mu^{TT,IF})) - 1) \times 100\%$	$(((\mu^{RR,RP})/(\mu^{RR,IF})) - 1) \times 100\%$
1	0.00	0.00
20	2.43	8.82
40	2.26	7.41
60	2.23	7.02
80	2.14	6.56
100	1.98	6.04
140	1.91	5.68
160	1.77	5.27
180	1.64	4.90
220	1.55	4.61
260	1.48	4.37
320	1.31	3.89

[a]N denotes the number of spherical subunits in the model. $\mu^{TT} = (1/3)\mathrm{Tr}(\mu^{TT})$ and $\mu^{RR} = (1/3)\mathrm{Tr}(\mu^{RR})$ (see eq 17).

of viscosity η. Formally, only the translational part (tt) is referred to as the Rotne–Prager tensor.[24,26] However, we mean the whole set of eqs 5–11 when we consider the mobility matrix in the RP approximation. While analytical expressions given with eqs 5–11 (and particularly the translational part, eqs 5 and 6) are often a basis of molecular simulations of systems of biological relevance,[1−3,6−9,13,28−31] it should be stressed that at the Rotne–Prager level only the far-field, two-body effects are accounted for. Consequently, translational (eq 5) and rotational (eq 7) self-mobilities of particles are not affected by the presence of other particles in the system. Moreover, translations and rotations of a given particle are not coupled (eq 9).

However, the fundamental difficulty inherent in evaluation of HI, namely their many-body-character, is addressed within the framework of the induced forces method (IF), a numerical scheme proposed by Cichocki and coauthors.[15] This scheme can be supplemented so that lubrication effects (that originate

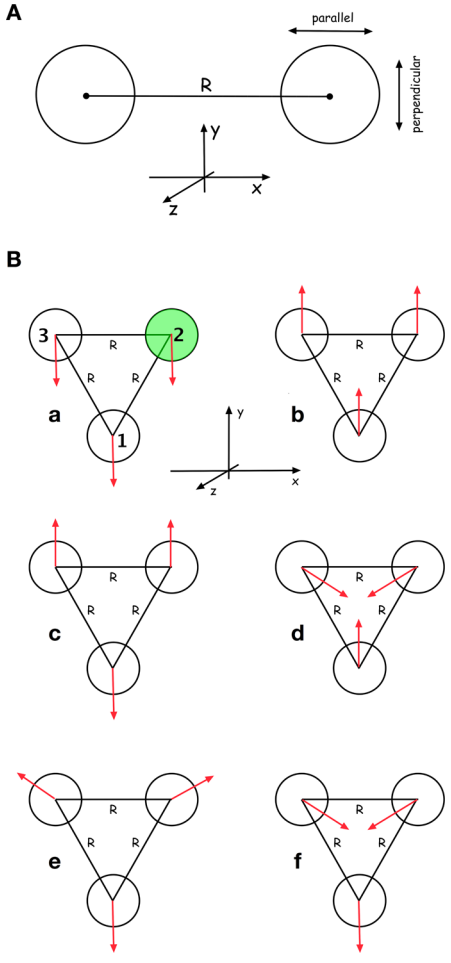

Figure 2. Configurations of objects in two (A) and three-body systems (B) considered in the current work. Red arrows in B: a–f denote directions of net direct forces applied to bodies.

from the strong velocity gradients of the flow field in the gap between particles at close separations) that contribute to relative motions of particles[15,32,35,36] are also taken into account

DOI: 10.1021/acs.jpcb.5b04675
J. Phys. Chem. B 2015, 119, 8425–8439

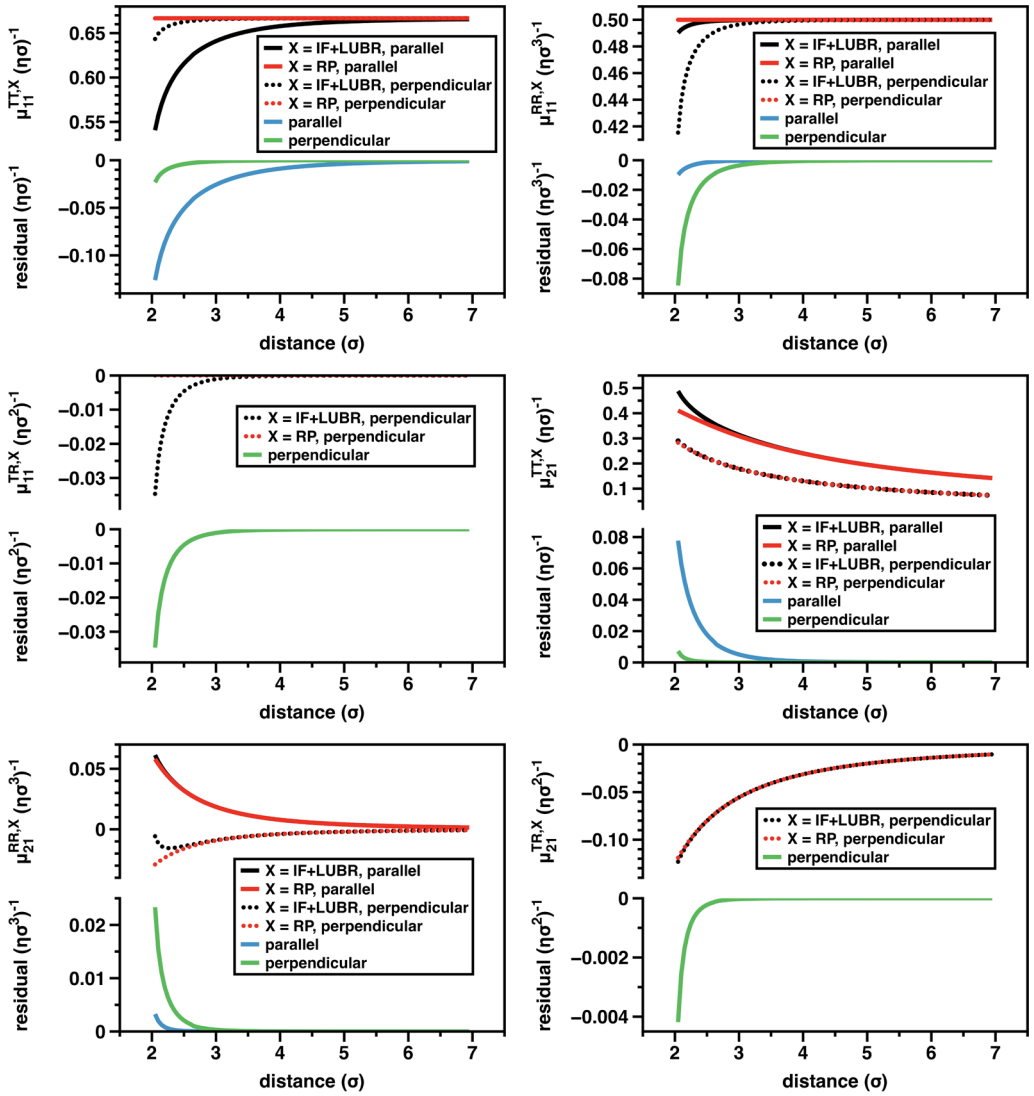

Figure 3. Mobilities (translational, *TT*; rotational, *RR*; and their couplings, *RT*) in the two-sphere system (Figure 1, left panel, A, and Figure 2A), calculated using either the induced forces method with the lubrication effects accounted for (IF + LUBR) or using the Rotne−Prager approximation (RP), as functions of the center-to-center distance of the spheres. σ denotes the hydrodynamic radius of spheres. Residuals (computed as point-by-point differences) of curves resulting from the two approaches used to model HI are also shown.

by means of a superposition of pair interactions.[15,36] An implementation of the IF method with lubrication corrections is included in the HYDROLIB library.[37] Particularly, HYDROLIB provides functions that can be used to evaluate the mobility matrix, $\boldsymbol{M}$ (eq 4), for a collection of equally sized spheres suspended in an incompressible viscous fluid.[37]

Techniques from the theory of low-Reynolds-number hydrodynamic interactions described above, can be easily applied to systems consisting of bodies that are made up of spheres which is a convenient way of representing complicated shapes of biological molecules.[20−22,33] For that, special types of constrained motion are considered,[18,38,39] which results in mobility matrices that correspond to translations, rotations (and their couplings) of conglomerates of spherical frictional elements, i.e., molecules.

As an illustration, let us consider an array (cluster, conglomerate) of N spherical elements. Once the complete $6N \times 6N$ mobility matrix of this system (eq 4) is known, the projection matrix, $\mathbf{C}$, can be used to obtain 6×6 mobility matrix of the cluster. In the considered case, the $6N \times 6$ projection matrix takes the form:

$$\mathbf{C} = \begin{pmatrix} \mathbf{1} & (\vec{r}_{CoG} - \vec{r}_1)\times \\ \cdots & \cdots \\ \mathbf{1} & (\vec{r}_{CoG} - \vec{r}_N)\times \\ \mathbf{0} & \mathbf{1} \\ \cdots & \cdots \\ \mathbf{0} & \mathbf{1} \end{pmatrix} \tag{15}$$

according to the condition that all spherical subunits in the array are rigidly connected so that they translate and rotate in concert. $\vec{r}_{i=1,\ldots,N}$ is a vector of Cartesian coordinates of the ith spherical subunit in the array, $\vec{r}_{CoG}$ denotes the location of the center of geometry of the array, and

$$(\vec{\mathbf{r}}_{CoG} - \vec{\mathbf{r}}_i) \times = \begin{pmatrix} 0 & -(z_{CoG} - z_i) & y_{CoG} - y_i \\ z_{CoG} - z_i & 0 & -(x_{CoG} - x_i) \\ -(y_{CoG} - y_i) & x_{CoG} - x_i & 0 \end{pmatrix} \tag{16}$$

DOI: 10.1021/acs.jpcb.5b04675
J. Phys. Chem. B 2015, 119, 8425−8439

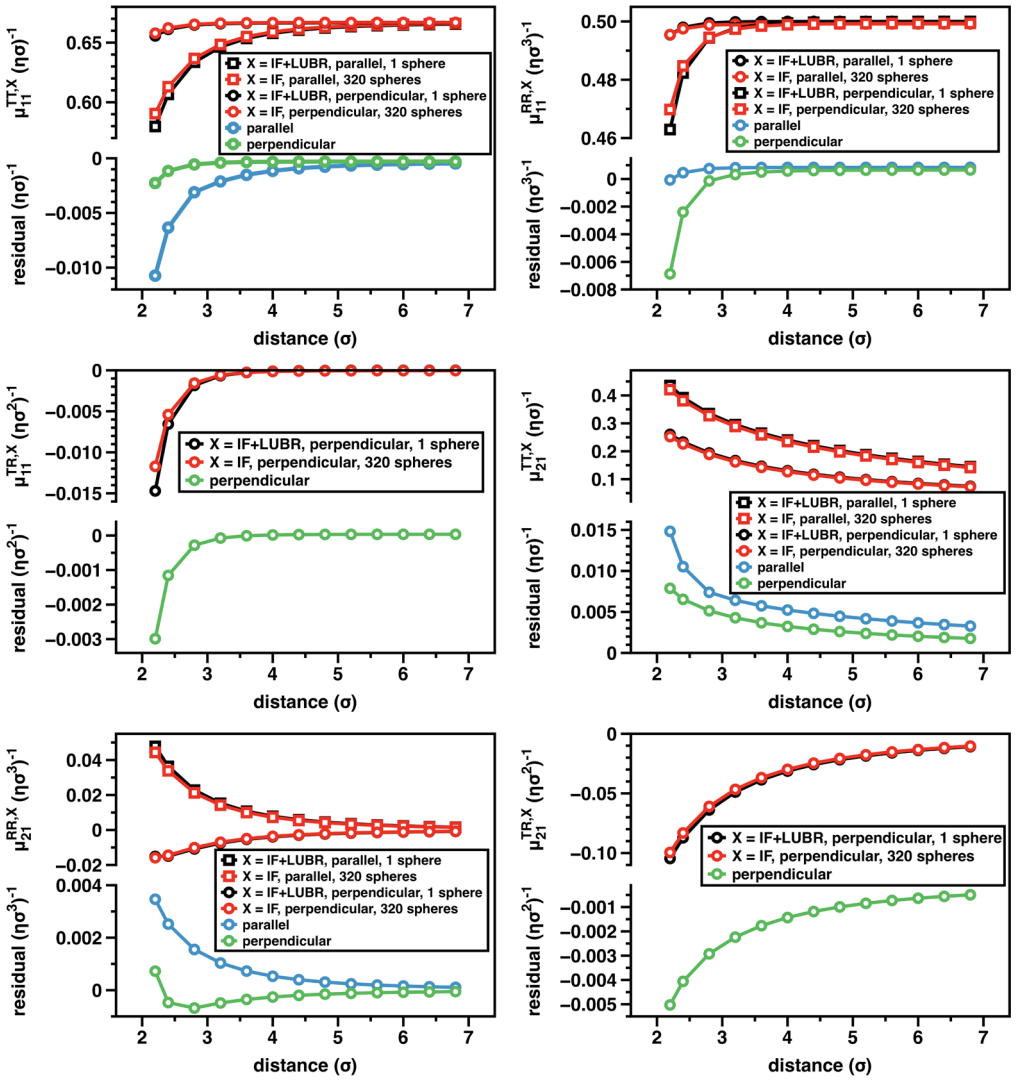

Figure 4. Mobilities (translational, *TT*; rotational, *RR*; and their couplings, *RT*) in the two-body system (Figure 2A) as functions of the center-to-center distance of the bodies. In the case of bodies modeled as single spheres (Figure 1, left panel, A), mobilities are evaluated based on the induced forces method and accounting for lubrication effects (IF + LUBR). In the case of bead-shell models consisting of 320 spherical elements (Figure 1, left panel, F), mobilities are evaluated based on the induced forces method and lubrication effects are not taken into account (IF). σ denotes the hydrodynamic radius of bodies. Residuals (computed as point-by-point differences) of corresponding curves obtained for different representations of bodies and different approaches to model their hydrodynamic properties and interactions are also shown.

The 6×6 mobility matrix of a rigid conglomerate of spherical subunits, $\boldsymbol{M}_C$, is given with

$$\mathbf{M}_C = (\mathbf{C}^T\mathbf{M}^{-1}\mathbf{C})^{-1} = \begin{pmatrix} \mu^{TT} & \mu^{TR} \\ \mu^{RT} & \mu^{RR} \end{pmatrix} \tag{17}$$

where the 3×3 mobility tensors $\mu^{\alpha\beta}$ correspond to the translational (TT) and rotational (RR) motions of the cluster and the hydrodynamic couplings between the translations and rotations (TR/RT).

The described procedure leading to rigid-body mobility matrices can be extended to systems containing any number, N_C, of separate rigid clusters (molecules) of spherical elements. In such a case, the projection matrix $\mathbf{C}$ is a $N_C \times N_C$ block matrix that consists of submatrices given with eq 17, corresponding to different clusters (C_i) located at the diagonal, and zeroes elsewhere:

$$\mathbf{C} = \begin{pmatrix} \mathbf{C}_1 & \mathbf{0} & \dots & \mathbf{0} & \mathbf{0} & \mathbf{0} \\ \mathbf{0} & \mathbf{C}_2 & \dots & \mathbf{0} & \mathbf{0} & \mathbf{0} \\ \dots & \dots & \dots & \dots & \dots & \dots \\ \mathbf{0} & \mathbf{0} & \dots & \mathbf{C}_i & \dots & \mathbf{0} \\ \dots & \dots & \dots & \dots & \dots & \dots \\ \mathbf{0} & \mathbf{0} & \dots & \mathbf{0} & \mathbf{0} & \mathbf{C}_{N_C} \end{pmatrix} \tag{18}$$

Resulting $6N_C \times 6N_C$ mobility matrix, $\boldsymbol{M}_{N_C}$ is formally equivalent to the matrix $\boldsymbol{M}$ given with eq 4:

$$\mathbf{M}_{N_C} = \begin{pmatrix} \mu_{11}^{TT} & \mu_{11}^{TR} & \dots & \mu_{1N_C}^{TT} & \mu_{1N_C}^{TR} \\ \mu_{11}^{RT} & \mu_{11}^{RR} & \dots & \mu_{1N_C}^{RT} & \mu_{1N_C}^{RR} \\ \dots & \dots & \dots & \dots & \dots \\ \dots & \dots & \dots & \dots & \dots \\ \mu_{N_C1}^{TT} & \mu_{N_C1}^{TR} & \dots & \mu_{N_CN_C}^{TT} & \mu_{N_CN_C}^{TR} \\ \mu_{N_C1}^{RT} & \mu_{N_C1}^{RR} & \dots & \mu_{N_CN_C}^{RT} & \mu_{N_CN_C}^{RR} \end{pmatrix} \tag{19}$$

DOI: 10.1021/acs.jpcb.5b04675
J. Phys. Chem. B 2015, 119, 8425−8439

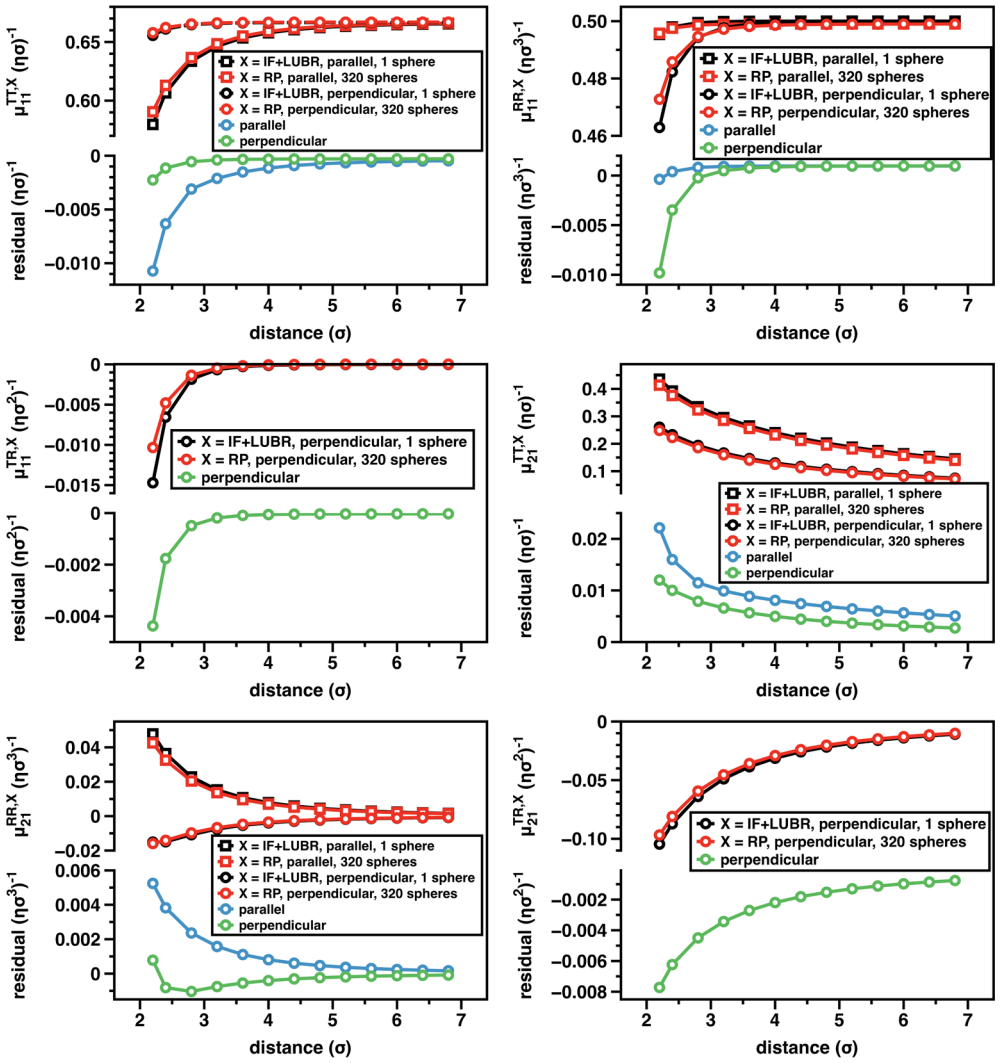

Figure 5. Mobilities (translational, *TT*; rotational, *RR*; and their couplings, *RT*) in the two-body system (Figure 2A) as functions of the center-to-center distance of the bodies. In the case of bodies modeled as single spheres (Figure 1, left panel, A), mobilities are evaluated based on the induced forces method and accounting for lubrication effects (IF + LUBR). In the case of bead-shell models consisting of 320 spherical elements (Figure 1, left panel, F), mobilities are evaluated based on the Rotne−Prager approximation (RP). σ denotes the hydrodynamic radius of bodies. Residuals (computed as point-by-point differences) of corresponding curves obtained for different representations of bodies and different approaches to model their hydrodynamic properties and interactions are also shown.

Tensors $\mu_{ii}^{\alpha\beta}$ correspond to translations (TT) and rotations (RR) of the ith cluster (molecule) and their couplings (TR/RT) that in general are affected by the presence of other clusters. Tensors $\mu_{ij,i\neq j}^{\alpha\beta}$ describe how motions of the ith cluster influence the motions of the j^{th} cluster.

Translational ($\vec{v}_i$) and rotational velocities ($\vec{\omega}_i$) of clusters are related to the net direct forces ($\vec{F}_i$) and torques ($\vec{T}_i$):

$$\begin{pmatrix} \vec{v}_1 \\ \vec{\omega}_1 \\ \cdots \\ \cdots \\ \vec{v}_{N_C} \\ \vec{\omega}_{N_C} \end{pmatrix} = \begin{pmatrix} \mu_{11}^{TT} & \mu_{11}^{TR} & \cdots & \mu_{1N_C}^{TT} & \mu_{1N_C}^{TR} \\ \mu_{11}^{RT} & \mu_{11}^{RR} & \cdots & \mu_{1N_C}^{RT} & \mu_{1N_C}^{RR} \\ \cdots & \cdots & \cdots & \cdots & \cdots \\ \cdots & \cdots & \cdots & \cdots & \cdots \\ \mu_{N_C1}^{TT} & \mu_{N_C1}^{TR} & \cdots & \mu_{N_CN_C}^{TT} & \mu_{N_CN_C}^{TR} \\ \mu_{N_C1}^{RT} & \mu_{N_C1}^{RR} & \cdots & \mu_{N_CN_C}^{RT} & \mu_{N_CN_C}^{RR} \end{pmatrix} \begin{pmatrix} \vec{F}_1 \\ \vec{T}_1 \\ \cdots \\ \cdots \\ \vec{F}_{N_C} \\ \vec{T}_{N_C} \end{pmatrix} \quad (20)$$

where forces are applied to centers of geometry of clusters, and torques are evaluated relative to centers of geometry of clusters.

We note that the procedure described above can be utilized regardless (is independent of) the method that is used to evaluate components of the input generalized mobility matrix $\boldsymbol{M}$ (eq 4).

Evaluation of Mobility Matrices. Generalized mobility matrices (eq 4) and rigid-body mobility matrices (eq 19) were evaluated based on the functions implemented in the HYDROLIB library[37] using the induced forces method either with or without lubrication corrections. In the case of calculations employing the Rotne−Prager approximation (eqs 5−11), generalized as well as rigid-body mobility matrices were evaluated using an in-house software.

Hydrodynamic Models. In the current work, we consider hydrodynamic effects in systems of spherically shaped bodies (molecules) modeled either as single spheres or as conglomerates of spherical subunits (bead-shell models[21]) in which the number of spherical subunits varies between 20 and 320 (Figure 1, left panel).

We use the following procedure to construct bead-shell models consisting of any number of spherical subunits.

DOI: 10.1021/acs.jpcb.5b04675
J. Phys. Chem. B 2015, 119, 8425−8439

We generate a given number of points equidistributed on the surface of a sphere, by choosing circles of latitude at constant intervals $L\theta$ and on these circles points with distances $L\phi$ such that $L\theta \simeq L\phi$, and that $L\theta \times L\phi$ equals the average area per point. These points are centers of spherical subunits constituting a bead-shell model (Figure 1, left panel). We require each of the spherical subunits positioned on the spherical surface to have an unit radius. We also require that there are no overlaps between subunits. We inflate the radius of the spherical surface on which spherical subunits are positioned to the minimal possible value that results in the fulfilment of these two conditions. All models were generated using an in-house software.

Right panel of Figure 1 shows values of hydrodynamic and excluded volume radii of conglomerates representing spherical molecules as functions of the number of spherical subunits. Hydrodynamic radii (Σ) can be derived from traces (Tr()) of appropriate rigid-body mobility tensors (eq 17) and relations given with eqs 13 and 14 as

$$\Sigma = \frac{1}{2\pi\eta \mathrm{Tr}(\mu^{TT})} \tag{21}$$

$$\Sigma = \left(\frac{1}{\frac{8}{3}\pi\eta \mathrm{Tr}(\mu^{RR})}\right)^{1/3} \tag{22}$$

We note that regardless the method used to evaluate μ^{TT} and μ^{RR} (i.e., either the IF method or the RP approach) and the number of spherical subunits in the conglomerate, differences in the values of the hydrodynamic radius that result from eqs 21 and 22 are negligible.

However, when we compare values of hydrodynamic radii resulting from calculations employing the IF method and the RP approximation with the excluded volume radii of conglomerates (the latter is defined as a sum of the radius of the spherical surface on which subunits are positioned and the unit radius of the spherical subunit), it can be seen that these two approaches give different results (Figure 1, right panel). As expected, in both cases, values of hydrodynamic radii obtained from both approaches converge to values of excluded volume radii with the increasing number of spherical subunits. For a conglomerate consisting of 320 subunits (which is the largest number that we consider), relative difference between the hydrodynamic radius resulting from the Rotne−Prager approach and the excluded volume radius is about 4% while in the case of the hydrodynamic radius derived using the induced forces method this difference is about 2% (Figure 1, right panel).

Comparison of translational and rotational self-mobilities of conglomerates resulting from calculations employing the Rotne−Prager approach and the induced forces method is presented in Table 1.

Differences of translational and rotational self-mobilities obtained with these two approaches decrease with the increasing number of spherical subunits. Overall, smaller differences are observed for translational mobilities. For the largest conglomerate considered here (320 spherical subunits), the relative difference between results obtained using the RP approach and the IF method is 1.3% in the case of translational mobility and 3.9% in the case of the rotational mobility.

Two and Three-Body Systems. We investigate hydrodynamic effects in two and three-body systems of spherical particles (Figure 2). Particles are modeled either using a single sphere (Figure 1, left panel, A) or as bead-shell models consisting of 320 spherical subunits (Figure 1, left panel, F).

For two-body systems, we evaluate the 12 × 12 rigid-body mobility matrices (eq 19) for different values of the bodies center-to-center distance. We analyze components of mobility matrices that correspond to relative motions of bodies in directions that are either parallel or perpendicular to the line connecting centers of bodies (Figure 2A).

In three-body systems centers of bodies are located at vertices of an equilateral triangle and 18 × 18 mobility matrices (eq 19) are evaluated for different values of triangle's side length (Figure 2B). Translational and rotational velocities resulting from application of unit forces with different directions to centers of bodies (eq 20, Figure 2B, parts a−f) are then analyzed. Forces are expressed in arbitrarily chosen units as mobility matrices are independent of this choice, and velocities are related linearly to forces (eq 20). We consider velocities of bodies rather than their mobilities, as the analysis performed in terms of components of a mobility matrix is in the case of a three-body system rather cumbersome. Additionally, the analysis of velocities shows the connection between our work and various simulation schemes.[12,13,32−34]

In two and three-sphere systems, the hydrodynamic radius of each sphere, σ, is set in all calculations to 1. In two and three-body systems consisting of bead-shell models, components TT, RR, and TR/RT of mobility matrices $\boldsymbol{M}_{N_C}$ (eq 19) are scaled by the value of the hydrodynamic radius of the bead-shell model raised to an appropriate power (Figure 1, right panel), so that they correspond to systems of spherical objects with unit hydrodynamic radii (σ). And as distances between bead-shell models are also appropriately scaled, we can compare directly results of different approaches to modeling of molecules and their hydrodynamic interactions.

In the following, values of translational mobilities are given in units of $((1)/(\eta\sigma))$, rotational mobilities in units of $((1)/(\eta\sigma^3))$, translational-rotational mobilities in units of $((1)/(\eta\sigma^2))$. Values of velocities are given in arbitrary units; translational velocities in units of v_o and rotational velocities in units of ω_o. Viscosity (η) in all calculations is set to $((1)/(4\pi))$.

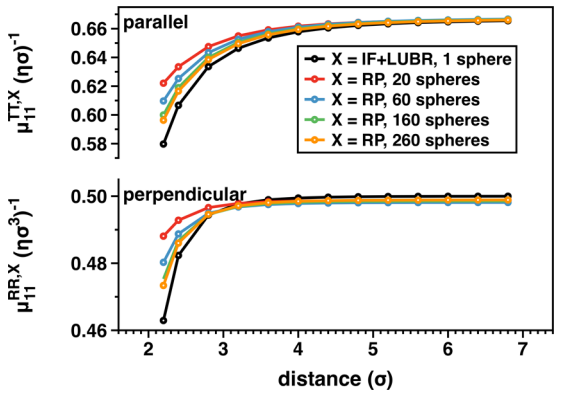

Figure 6. Components of self-mobilities (translational, TT, and rotational, RR) in the two-body system as functions of the center-to-center distance of bodies. In the case of bodies modeled as single spheres, mobilities are evaluated based on the induced forces method and accounting for lubrication effects (IF + LUBR). In the case of bead-shell models consisting of N (with N set respectively to 20, 60, 160, and 260) spherical elements, mobilities are evaluated based on the Rotne−Prager approximation (RP). σ denotes the hydrodynamic radius of bodies.

DOI: 10.1021/acs.jpcb.5b04675
J. Phys. Chem. B 2015, 119, 8425−8439

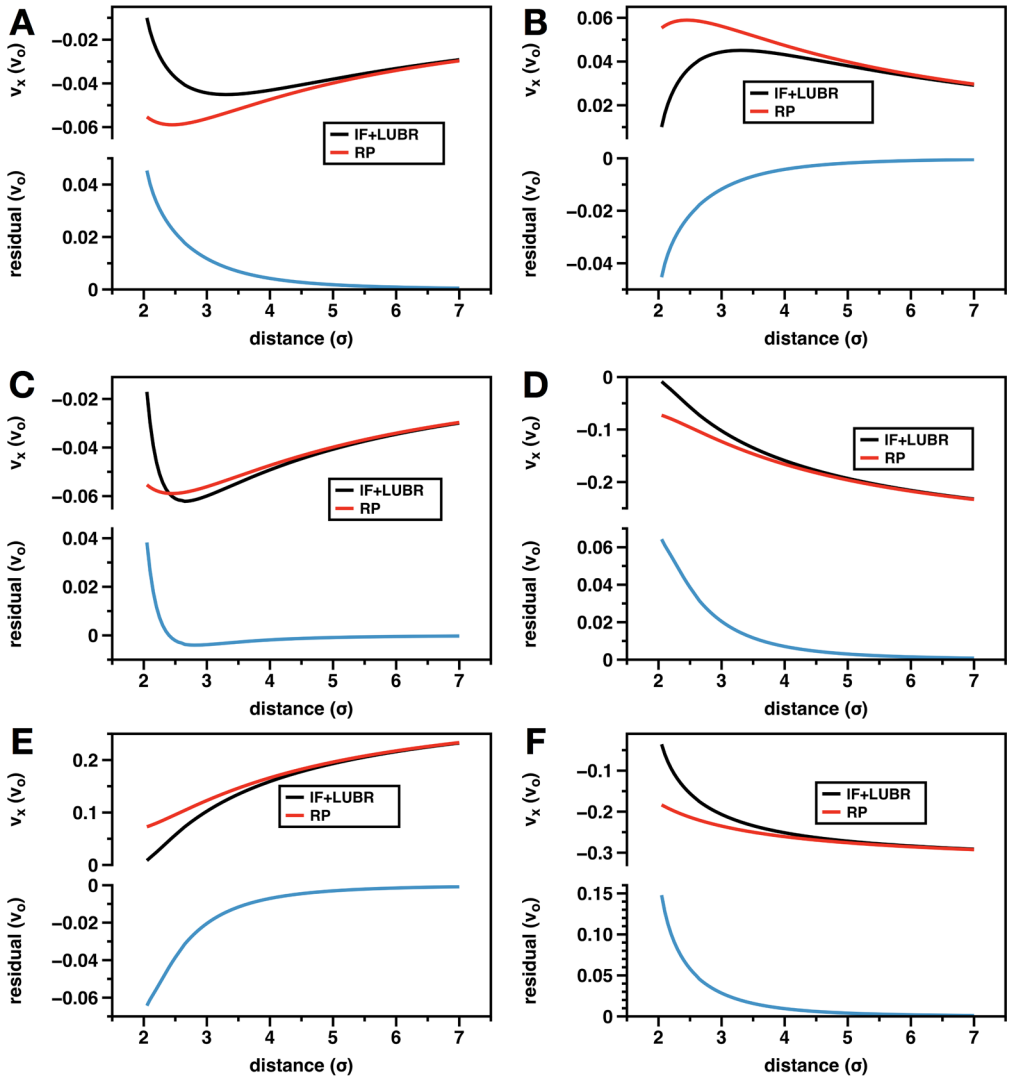

Figure 7. x-component of the translational velocity (v_x) of the second (denoted with the green color) sphere in Figure 2B as a function of the distance (side length of an equilateral triangle in Figure 2B) between spheres in three-sphere systems. Objects are modeled as single spheres (Figure 1, left panel, A). Presented curves result either from the calculations based on the induced forces method with lubrication corrections accounted for (IF + LUBR) or based on the Rotne−Prager approach (RP). σ is the hydrodynamic radius of spheres. Residuals of corresponding curves, computed as point-by-point differences, are also shown. Subfigures A−F correspond to cases (directions of forces acting on bodies) a−f from Figure 2B.

RESULTS

Mobilities in Two-Body Systems. For the sake of illustration, we first consider a system consisting simply of two spheres (Figure 1A). In general, the dynamics in a two-sphere system can be described in terms of motions that are either parallel or perpendicular to the line connecting centers of spheres[35,41] (Figure 2A).

Two-sphere mobilities (evaluated using either the Rotne−Prager approximation or the induced forces method corrected for lubrication effects) that correspond to parallel and perpendicular motions, are shown in Figure 3 as functions of the center-to-center distance of spheres. Clearly, the Rotne−Prager approach fails to correctly describe dynamics in the two-sphere system for interparticle distances below 3σ (with σ being the hydrodynamic radius of spheres) (Figure 3). Additionally, the RP approach results in translational and rotational self-mobilities ($\mu_{11}^{TT,RP}$ and $\mu_{11}^{RR,RP}$ in Figure 3) that are identical to the corresponding single-sphere values (eqs 13 and 14), while self-mobilities obtained using the IF method are distance-dependent. Rotne−Prager approach results in the absence of self-coupling of translations and rotations ($\mu_{11}^{TR,RP}$ in Figure 3). Lubrication corrections play a role close to contact, at interparticle distances close to 2σ, which is evident in particular in plots of perpendicular components of μ_{21}^{RR} and parallel components of μ_{21}^{TT} in Figure 3 (see also Figure S1, Supporting Information).

In the second system that we consider, each sphere is replaced with a bead-shell model of 320 frictional elements representing a spherical molecule (Figure 1, left panel, F). We evaluate mobilities in such a two-body system employing the IF method (without lubrication corrections) for different distances between geometry centers of molecules. Mobility components corresponding to parallel and perpendicular motions obtained in this case are shown in Figure 4, together with mobilities obtained for the system consisting of two spheres using the IF method with lubrication corrections accounted for. The two approaches applied to model spherical molecules (i.e., either explicitly using a single sphere per molecule or using bead-shell models) result in similar dynamics in the studied system. Even though lubrication corrections are neglected in the evaluation of mobilities of bead-shell models, this affects results only

DOI: 10.1021/acs.jpcb.5b04675
J. Phys. Chem. B 2015, 119, 8425−8439

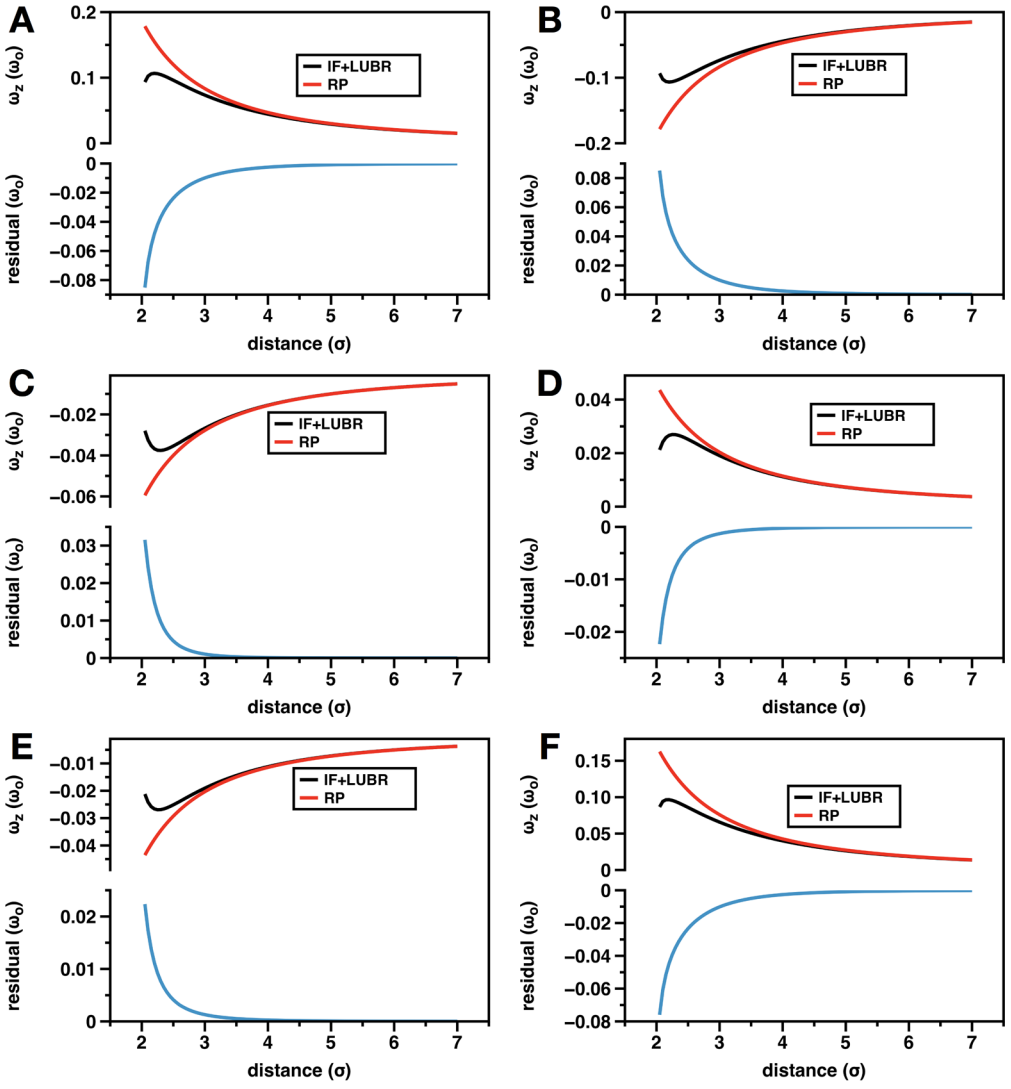

Figure 8. z-component of the rotational velocity (ω_z) of the second (shown with the green color) sphere in Figure 2B as a function of the distance (side length of an equilateral triangle in Figure 2B) between spheres in three-sphere systems. Objects are modeled as single spheres (Figure 1, left panel, A). Presented curves result either from the calculations based on the induced forces method with lubrication corrections (IF + LUBR) or based on the Rotne−Prager approach (RP). Here, σ is the hydrodynamic radius of spheres. Residuals of corresponding curves, computed as point-by-point differences, are also shown. Subfigures A−F correspond to cases (directions of forces acting on bodies) a−f from Figure 2B.

slightly. As we stated above, lubrication effects come into play at close distances, for almost touching bodies. Spheres in our calculations are replaced with conglomerates of much smaller spherical elements and lubrication corrections are evaluated in a pairwise manner;[15,36] their magnitudes depend on the size of the interacting bodies. As a consequence, the effect of lubrication corrections on the dynamics in the system of bead-shell models is not significant.

We may now consider the same system, but evaluate mobilities of bead-shell models employing the Rotne−Prager approximation (eqs 5−11) instead of the induced force method. This leads to functions of interparticle distances that are shown in Figure 5), which we again compare with functions obtained using the IF method with lubrication corrections for the system consisting of two spheres.

While the Rotne−Prage approximation fails to describe correctly the dynamics in the two-sphere system (Figure 3), it performs reasonably well when spheres are replaced with bead-shell models consisting of multiple frictional elements. Moreover, its performance in the studied case of bead-shell models is only slightly inferior to the performance of the induced forces method (see Figure 4). We note that the larger the number of frictional elements used in bead-shell models, the better the accuracy of results obtained with the RP approach, not only in the case of single molecules that we have described above (Table 1) but also in two-body systems. This is illustrated in Figure 6 for the μ_{11}^{TT} and μ_{11}^{RR} mobility components.

One may compare curves shown in Figure 6 with corresponding curves obtained using the same approach for the two-sphere system (Figure 3). Replacing spheres with bead-shell models causes that their translational and rotational self-mobilities are no longer described with eqs 13 and 14 that correspond to translational and rotational mobilities of a single sphere. Instead, translational and rotational self-mobilities in the two-body system of bead-shell models evaluated using the Rotne−Prager approach become dependent on the distance between bodies.

Dynamics in Three-Body Systems. At the beginning of the previous section we have demonstrated the commonly recognized failure of the Rotne−Prager approach in describing

DOI: 10.1021/acs.jpcb.5b04675
J. Phys. Chem. B 2015, 119, 8425−8439

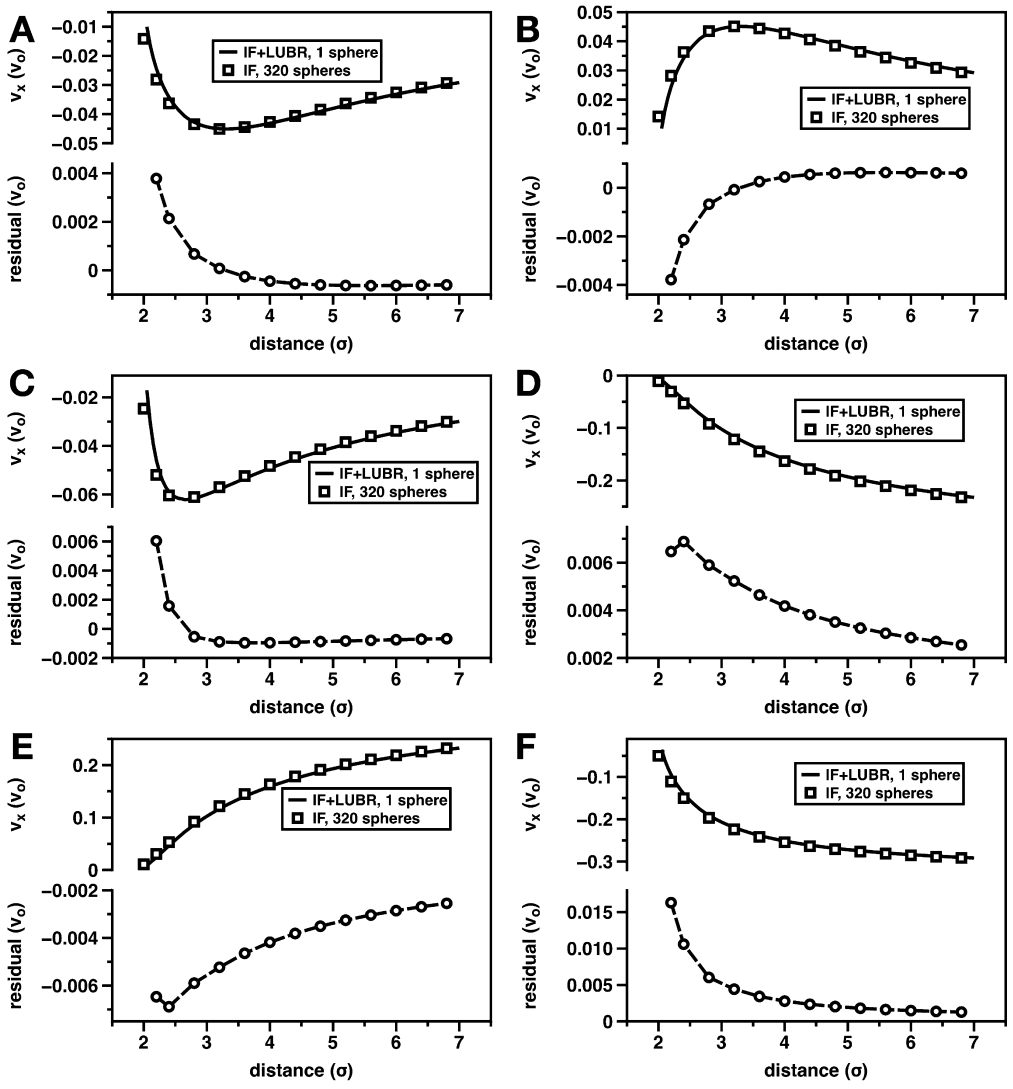

Figure 9. x-component of the translational velocity (v_x) of the second body (shown with the green color) in Figure 2B as a function of the distance (side length in a equilateral triangle in Figure 2B) between bodies in the three-body system. Objects are modeled either as single spheres (Figure 1, left panel, A) or as conglomerates of 320 spherical subunits (Figure 1, left panel, F). In the former case presented curves result from the calculations based on the induced forces method with lubrication corrections (IF+LUBR). In the latter case the induced forces method without lubrication corrections (IF) was employed. σ is the hydrodynamic radius of bodies. Residuals of corresponding curves, computed as point-by-point differences, are also shown. Subfigures A–F correspond to cases (directions of forces acting on bodies) a–f from Figure 2B.

the dynamics in the two-sphere system (Figure 3). We now investigate the three-sphere system. As we have described above, we analyze the dynamics in three-body systems in terms of translational and rotational velocities that arise when direct forces (but no torques) are applied to bodies (Figure 2B).

In Figures 7 and 8 we show components of the translational (v_x) and rotational (ω_z) velocities, (see also Figures S2–S4 in Supporting Information that depict remaining velocity components resulting from applied forces) of one of the spheres in the system consisting of three equal spheres positioned at vertices of an equilateral triangle (Figure 2B), as functions of the triangle's side length. Velocities were calculated based on eq 3, with mobility matrices evaluated either using the induced forces method with the lubrication correction, or using the Rotne–Prager approximation. Again, the failure of the RP approach is evident. When distances between the spheres are smaller than 4σ in the case of translational velocities or 3σ in the case of rotational velocities, curves resulting from the induced forces method and the Rotne–Prager approach diverge significantly. Notably, in the case of the ω_z component of the rotational velocity, differences between curves resulting from these two approaches are not only quantitative but also qualitative. Unlike curves obtained using the Rotne–Prager approximation, ω_z curves resulting from the application of the induced forces approach are nonmonotonic for distances below 3σ (Figure 8).

Let us now consider, in a similar fashion, the translational and rotational dynamics of a body in the three-body system (Figure 2B), consisting of identical bead-shell models of spherical molecules (Figure 1F). In Figures 9 and 10, we show the components of translational and rotational velocities of one of the bodies in the systems consisting of either three spheres or three bead-shell models of spherical molecules. In the former case mobility matrices needed to evaluate velocities are calculated using the induced forces method with the lubrication correction. In the latter case, mobilities are evaluated using the induced forces method, but without taking into account lubrication effects.

DOI: 10.1021/acs.jpcb.5b04675
J. Phys. Chem. B 2015, 119, 8425–8439

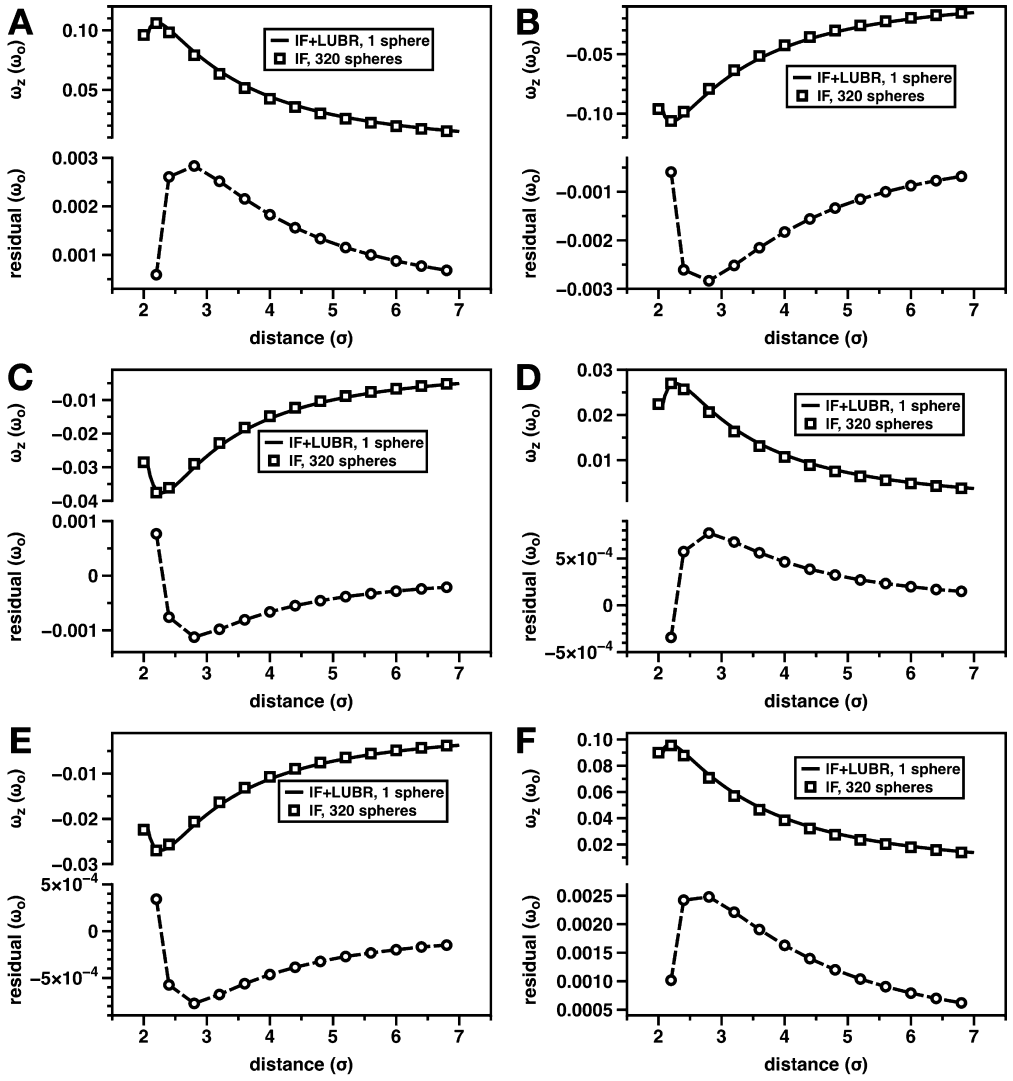

Figure 10. z-component of the rotational velocity (ω_z) of the second body (shown with the green color) in Figure 2B as a function of the distance (side length in a equilateral triangle in Figure 2B) between bodies in the three-body system. Objects are modeled either as single spheres (Figure 1, left panel, A) or as conglomerates of 320 spherical subunits (Figure 1, left panel, F). In the former case presented curves result from the calculations based on the induced forces method with lubrication corrections (IF+LUBR). In the latter case the induced forces method without lubrication corrections (IF) was employed. σ is the hydrodynamic radius of bodies. Residuals of corresponding curves, computed as point-by-point differences, are also shown. Subfigures A–F correspond to cases (directions of forces acting on bodies) a–f from Figure 2B.

As could be expected, representing the bodies with bead-shell models results in this case in the correct description of the dynamics in the studied systems. Discrepancies in velocities resulting from the two approaches used to model spherical molecules, that we observe for distances close to 2σ, result mainly from the fact that we purposely neglect pairwise lubrication corrections to interactions between frictional elements that constitute the bead-shell models.

More interesting are however results that we present in Figures 11 and 12, namely, the components of translational and rotational velocities of one of the bodies in three-body systems from Figure 2B, consisting of bead-shell models of spherical particles (Figure 1F), evaluated using the Rotne–Prager approach. It is clear from the plots given in these figures, that the RP approach performs almost equally well as the induced forces approach, when applied to model the hydrodynamics in three-body systems in which bodies are described using bead-shell models.

DISCUSSION

Common way in which hydrodynamic effects in complex biological systems are investigated is through particle-based Brownian dynamics simulations.[13] In most of such studies, HI are evaluated using the Rotne–Prager tensor and its extensions,,[24−26] at the far-field, two-body level. Pairwise calculations of the RP tensor with its relatively simple analytic form can be easily and effectively incorporated in serial and parallel codes of molecular simulations software.[42,43] However, the calculation of correlated Brownian noise vectors in Brownian dynamics simulations is computationally very demanding task as it requires the mobility matrix of the simulated system, evaluated at the Rotne–Prager level of theory, to be inverted at each simulation step, an operation that scales as $O(N^3)$ where N is the number of spherical frictional elements in the system. Thus, it is understandable that studies that aim at testing and improving approaches to model hydrodynamic interactions in biological context focus usually on decreasing their computational cost by proposing various alternatives to the

DOI: 10.1021/acs.jpcb.5b04675
J. Phys. Chem. B 2015, 119, 8425–8439

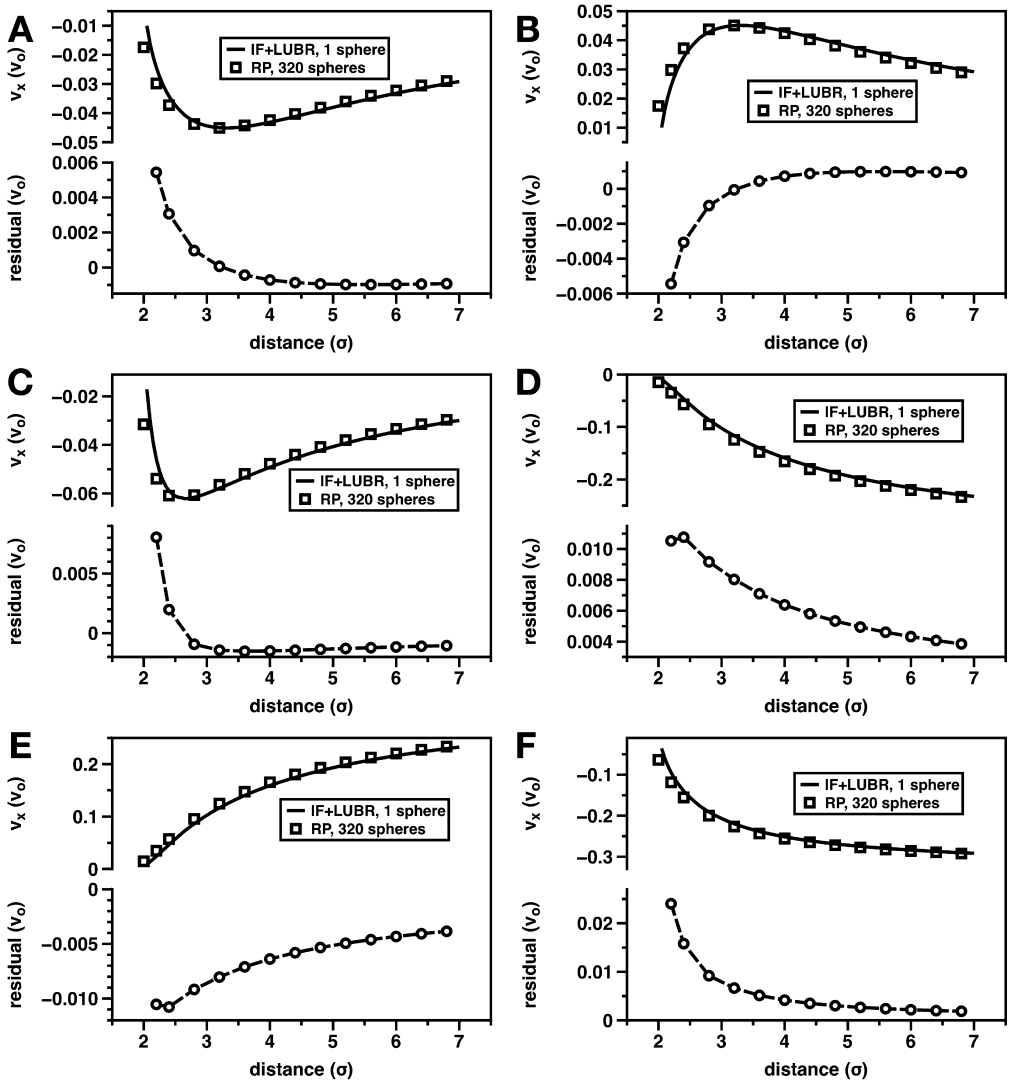

Figure 11. x-component of the translational velocity (v_x) of the second body (shown with the green color) in Figure 2B as a function of the distance (side length in a equilateral triangle in Figure 2B) between bodies in the three-body system. Objects are modeled either as single spheres (Figure 1, left panel, A) or as conglomerates of 320 spherical subunits (Figure 1, left panel, F). In the former case presented curves result from the calculations based on the induced forces method with lubrication corrections accounted for (IF + LUBR). In the latter case, the Rotne−Prager approach (RP) was employed. σ is the hydrodynamic radius of bodies. Residuals of corresponding curves, computed as point-by-point differences, are also shown. Subfigures A−F correspond to cases (directions of forces acting on bodies) a−f from Figure 2B.

direct inversion of large matrices[44−46] or by applying coarse-graining procedures.[19,28]

Our aim is different as we question and examine the applicability of the Rotne−Prager approach to model effects of HI in biological systems. We believe, that hydrodynamic interactions must be considered carefully in order to obtain physically meaningful picture of biological processes. Reliable estimation of errors introduced by employing approximations to model effects of HI is needed. This might help us to introduce necessary modifications to reduce eventual errors to acceptable level. We apply the RP approach to calculate self-mobilities of rigid molecules and to evaluate the translational and rotational dynamics in two and three-body systems. As a reference, we choose an accurate numerical scheme that accounts for the many-body character of HI and for effects originating from strong velocity gradients of the flow field in the gap between approaching molecules.[15]

Considering the evaluation of rigid-body mobility tensors of molecules, we show quantitatively, how the accuracy of the two-body, far-field Rotne−Prager approach increases with the increasing number of frictional elements in the bead model of a molecule (Table 1, Figure 1). When spherical molecules are modeled using 20 frictional elements, relative differences of translational and rotational self-mobilities obtained using the two-body RP approach and the IF method are ∼2.5% and ∼8.8%, respectively. When the number of elements in the model is increased to 320, differences in self-mobilities decrease respectively to ∼1.3% and ∼3.9%. We note that lubrication plays no role in evaluation of rigid-body mobility tensors of isolated macromolecules, as there are no relative motions between frictional elements in bead models (Table 1). Thus, these differences result from the fact that the higher order, many-body terms are neglected in the Rotne−Prager approximation.[24,26] This result should not be dismissed without any concern, as usually rigid-body hydrodynamic calculations, that allow one to describe diffusional properties of molecules in dilute solutions are conducted using the two-body, far field approximation.[20−23] Moreover, two-body approximations are

DOI: 10.1021/acs.jpcb.5b04675
J. Phys. Chem. B 2015, 119, 8425−8439

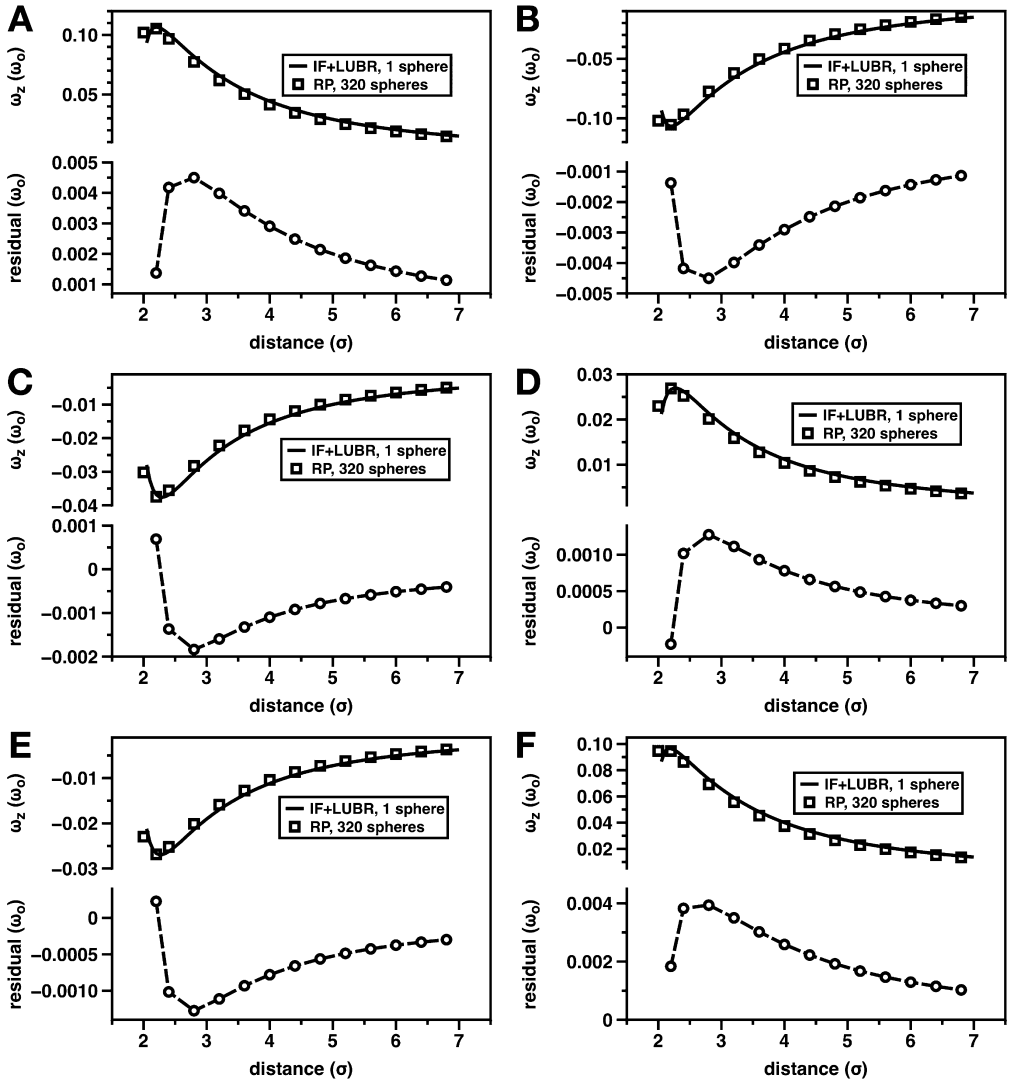

Figure 12. z-component of the rotational velocity (ω_z) of the second body (shown with the green color) in Figure 2B as a function of the distance (side length in a equilateral triangle in Figure 2B) between bodies in the three-body system. Objects are modeled either as single spheres (Figure 1, left panel, A) or as conglomerates of 320 spherical subunits (Figure 1, left panel, F). In the former case presented curves result from the calculations based on the induced forces method with lubrication corrections taken into account (IF + LUBR). In the latter case the Rotne−Prager approach (RP) was employed. σ is the hydrodynamic radius of bodies. Residuals of corresponding curves, computed as point-by-point differences, are also shown. Subfigures A−F correspond to cases (directions of forces acting on bodies) a−f from Figure 2B.

used also in studies of hydrodynamic effects on the folding/unfolding and solution conformation of proteins in which proteins are represented with coarse-grained models consisting of spherical elements (beads or pseudoatoms).[6−8] And while lubrication effects in such systems can probably be safely neglected as relative motions of frictional elements within models are limited by intramolecular bonded potentials, effects resulting from the many-body character of HI and terms of order higher than $(((\sigma)/(r_{ij})))^3$ (which is the order to which the RP treatment of HI is exact) in power series of the inverse of interparticle distances used to represent mobility matrices are bound to play a role.

We examine the performance of the Rotne−Prager approach when applied to describe the translational and rotational dynamics in two and three-body systems consisting of either spheres or bead-shell models of spherical molecules. In the former case we illustrate the failure (quantitative as well as qualitative) of the Rotne−Prager approach to correctly describe dynamics in two and three-sphere systems (Figures 3, 7, and 8) at separations that are comparable to spheres' size. In the latter case, when spheres are replaced with bead-shell models, the application of the Rotne−Prager approach results in correct translational and rotational dynamics in two and three-body systems (Figures 5, 11, and 12) for intermolecular distances ranging from large separation up to the closest approach allowed by the excluded volume effects.

Hydrodynamic effects can be evaluated in the considered systems of spherical molecules at two levels. In two and three-body systems there are many-body hydrodynamic interactions between frictional elements that constitute hydrodynamic models. In two and three-body systems hydrodynamic effects can be also considered at the whole-body level. Evaluation of hydrodynamic interactions between large number of frictional elements that constitute bodies should recreate hydrodynamic effects calculated at the whole-body level, both in the two and three-body systems. However, this only holds true for the induced forces approach (Figures 4, 9 and 10). The failure of the RP approach to correctly describe dynamics in two and

DOI: 10.1021/acs.jpcb.5b04675
J. Phys. Chem. B 2015, 119, 8425−8439

three-sphere systems for intermolecular distances of the order of spheres' size and the fact that in this regime it leads to physically sound results only when spheres are replaced with hydrodynamic models consisting of sufficiently large number of elements, seem to contradict the recently described idea of modeling systems of many flexible biological molecules[28] in which hydrodynamic interactions are separated into intra- and intermolecular terms. The former are evaluated using coarse-grained hydrodynamic bead models of molecules, the latter are evaluated assuming that molecules are spherical. Both types of interactions are modeled using the modified form of the Rotne−Prager level of theory.[28]

Although our current study is limited to systems consisting of spherical molecules, we use the term *biological systems*, as the bead modeling approach that we employ is in general able to account for complicated shapes of interacting objects, rigid as well as flexible, and thus we deem the conclusions of our work to be universal and of importance for studies on biological macromolecules.

■ ASSOCIATED CONTENT

Supporting Information

Mobility components in the two-sphere system, evaluated using the induced forces method with and without lubrication corrections (Figure S1) and *y*-components of the translational velocity (v_y) of one of the bodies in three-body systems from Figure 2B obtained using different methods of HI calculations and for different models of spherical particles (Figures S2−S4). The Supporting Information is available free of charge on the ACS Publications website at DOI: 10.1021/acs.jpcb.5b04675.

■ AUTHOR INFORMATION

Corresponding Author

*(M.D.) Telephone: +48 22 5543 692 Fax: +48 22 5540 801 E-mail: mdlugosz@cent.uw.edu.pl.

Notes

The authors declare no competing financial interest.

■ ACKNOWLEDGMENTS

The authors acknowledge support from National Science Centre (UMO-2014/13/B/NZ1/00004).

■ REFERENCES

(1) Frembgen-Kesner, T.; Elcock, A. H. Absolute Protein-Protein Association Rate Constant from Flexible, Coarse-Grained Brownian Dynamics Simulations: the Role of Intermolecular Hydrodynamic Interactions in Barnase-Barstar Association. *Biophys. J.* **2010**, *99*, L75−L77.

(2) Antosiewicz, J.; McCammon, J. A. Electrostatic and Hydrodynamic Orientational Steering Effects in Enzyme-Substrate Association. *Biophys. J.* **1995**,*69*.

(3) Antosiewicz, J.; Briggs, J. M.; McCammon, J. A. Orientational Steering in Enzyme-Substrate Association: Ionic Strength Dependence of Hydrodynamic Torque Effects. *Eur. Biophys. J.* **1996**, *24*, 137−141.

(4) Brune, D.; Kim, S. Hydrodynamic Steering Effects in Protein Association. *Proc. Natl. Acad. Sci. U.S.A.* **1994**, *91*, 2930−2934.

(5) Długosz, M.; Antosiewicz, J. M. Hydrodynanamic Effects on the Relative Rotational Velocity of Associating Proteins. *J. Phys. Chem. B* **2013**, *117*, 6167−6174.

(6) Szymczak, P.; Cieplak, M. Influence of Hydrodynamic Interactions on Mechanical Unfolding of Proteins. *J. Phys.: Condens. Matter* **2007**, *19*, 285224−285236.

(7) Szymczak, P.; Cieplak, M. Proteins in Shear Flow. *J. Chem. Phys.* **2007**, *127*, 155106−155113.

(8) Frembgen-Kesner, T.; Elcock, A. H. Striking Effects of Hydrodynamic Interactions on the Simulated Diffusion and Folding of Proteins. *J. Chem. Theory Comput.* **2009**, *5*, 242−256.

(9) Ando, T.; Skolnick, J. On the Importance of Hydrodynamic Interactions in Lipid Membrane formation. *Biophys. J.* **2013**, *104*, 96−105.

(10) Mereghetti, P.; Wade, R. C. Atomic Detail Brownian Dynamics Simulations of Concentrated Protein Solutions with a Mean Field Treatment of Hydrodynamic Interactions. *J. Phys. Chem. B* **2012**, *116*, 8523−8533.

(11) Ando, T.; Skolnick, J. Crowding and Hydrodynamic Interactions Likely Dominate In Vivo Macromolecular Motion. *Proc. Natl. Acad. Sci. U.S.A.* **2010**, *107*, 18457−18462.

(12) Bossis, G.; Brady, J. F. Stokesian Dynamics. *Annu. Rev. Fluid. Mech.* **1988**, *20*, 111−157.

(13) Ermak, D. L.; McCammon, J. A. Brownian Dynamics with Hydrodynamic Interactions. *J. Chem. Phys.* **1978**, *69*, 1352−1360.

(14) Mazur, P.; van Sarloos, W. Many-Sphere Hydrodynamic Interactions and Mobilities in a Suspension. *Physica A* **1982**, *115*, 21−57.

(15) Cichocki, B.; Felderhof, B. U.; Hinsen, K.; Wajnryb, E.; Bławździewicz, J. Friction and Mobility of Many Spheres in Stokes Flow. *J. Chem. Phys.* **1994**, *100*, 3780−3790.

(16) Felderhof, B. U. Many-Body Hydrodynamic Interactions in Suspensions. *Physica A* **1988**, *151*, 1−16.

(17) Brenner, H. Coupling Between the Translational and Rotational Brownian Motions of Rigid Particles of Arbitrary Shape. *J. Colloid.Sci.* **1965**, *20*, 104−122.

(18) Cichocki, B.; Hinsen, K. Stokes Drag on Conglomerates of Spheres. *Phys. Fluids* **1995**, *7*, 285−291.

(19) Wang, N.; Huber, G. A.; McCammon, J. A. Assessing the Two-Body Diffusion Tensor Calculated by the Bead Model. *J. Chem. Phys.* **2013**, *138*, 204117−8.

(20) García de la Torre, J. Building Hydrodynamic Bead-shell Models for Rigid Bioparticles of Aribtrary Shape. *Biophys. Chem.* **2001**, *94*, 265−274.

(21) Carrasco, B.; García de la Torre, J. Hydrodynamic Properties of Rigid Particles: Comparison of Different Modeling and Computational Procedures. *Biophys. J.* **1999**, *76*, 3044−3057.

(22) García de la Torre, J.; Bernadó, P.; Pons, M. Hydrodynamic Models and Computational Methods for NMR Relaxation. *Methods Enzymol.* **2005**, *394*, 419−430.

(23) García de la Torre, J.; Huertas, M. L.; Carrasco, B. Calculation of Hydrodynamic Properties of Globular Proteins from their Atomic Level Structure. *Biophys. J.* **2000**, *78*, 719−730.

(24) Rotne, J.; Prager, S. Variational Treatment of Hydrodynamic Interaction in Polymers. *J. Chem. Phys.* **1969**, *50*, 4831−4837.

(25) Yamakawa, H. Transport Properties of Polymer Chains in Dilute Solution: Hydrodynamic Interaction. *J. Chem. Phys.* **1970**, *53*, 436−443.

(26) Wajnryb, E.; Mizerski, K. A.; Zuk, P. J.; Szymczak, P. Generalization of the Rotne-Prager-Yamakawa Mobility and Shear Disturbance Tensors. *J. Fluid. Mech.* **2013**, *731*, R3.

(27) Zuk, P. J.; Wajnryb, E.; Mizerski, K. A.; Szymczak, P. Rotne-Prager-Yamakawa Approximation for Different-Sized Particles in Application to Macromolecular Bead Models. *J. Fluid. Mech.* **2014**, *741*, R5.

(28) Elcock, A. Molecule-Centered Method for Accelerating the Calculation of Hydrodynamic Interactions in Browniand Dynamics Simulations Containing Many Flexible Molecules. *J. Chem. Theory Comput.* **2013**, *9*, 3224−3239.

(29) Ando, T.; Skolnick, J. Sliding of Proteins Non-Specifically Bound to DNA: Brownian Dynamics Studies with Coarse-Grained Protein and DNA Models. *PLoS Comput. Biol.* **2014**, *10*, e1003990.

(30) Florescu, A.-M.; Joyeux, M. Description of Nonspecific DNA-Protein Interaction and Facilitated Diffusion with a Dynamical Model. *J. Chem. Phys.* **2009**, *130*, 015103.

DOI: 10.1021/acs.jpcb.5b04675
J. Phys. Chem. B 2015, 119, 8425−8439

(31) Gorba, C.; Helms, V. Diffusional Dynamics of Cytochrome C Molecules in the Presence of a Charged Surface. *Soft Mater.* **2003**, *1*, 185−202.
(32) Bossis, G.; Brady, J. F. Dynamic Simulation of Sheared Suspensions. I. General Method. *J. Chem. Phys.* **1984**, *80*, 5141−5155.
(33) Fernandes, M. X.; García de la Torre, J. Brownian Dynamics Simulations of Rigid Particles of Arbitrary Shape in External Fields. *Biophys. J.* **2002**, *83*, 3039−3048.
(34) Allison, S. A. Brownian Dynamics Algorithm for Arbitrary Rigid Bodies - Application to Polarized Dynamic Light-Scattering. *Macromolecules* **1991**, *24*, 530−536.
(35) Jeffrey, D. J.; Onishi, Y. Calculation of the Resistance and Mobility Functions for two Unequal Rigid Spheres in Low-Reynolds-Number Flow. *J. Fluid. Mech.* **1984**, *139*, 261−290.
(36) Durlofsky, L.; Brady, J. F.; Bossis, G. Dynamic Simulation of Hydrodynamically Interacting Particles. *J. Fluid Mech.* **1987**, *180*, 21−49.
(37) Hinsen, K. HYDROLIB: A Library for the Evaluation of Hydrodynamic Interactions in Colloidal Suspensions. *Comput. Phys. Commun.* **1995**, *88*, 327−340.
(38) García Bernal, J. M.; García de la Torre, J. Transport Properties and Hydrodynamic Centers of Rigid Macromolecules with Arbitrary Shapes. *Biopolymers* **1980**, *19*, 751−766.
(39) Harvey, S. C.; García de la Torre, J. Coordinate System for Modeling of the Hydrodynamic Resistance and Diffusion Coefficients of Irregularly Shaped Rigid Molecules. *Macromolecules* **1980**, *13*, 960−964.
(40) Humphrey, W.; Dalke, A.; Schulten, K. VMD - Visual Molecular Dynamics. *J. Mol. Graphics* **1996**, *14*, 33−38.
(41) Batchelor, G. K. Brownian Diffusion of Particles with Hydrodynamic Interaction. *J. Fluid Mech.* **1976**, *74*, 1−29.
(42) Długosz, M.; Zieliński, P.; Trylska, J. Brownian Dynamics Simulations on CPU and GPU with BD_BOX. *J. Comput. Chem.* **2011**, *32*, 2734−2744.
(43) García de la Torre, J.; Hernández Cifre, J. G.; Ortega, A.; Pérez Sánchez, H. E.; Pamies, R. SIMUFLEX: Algorithms and Tools for Simulation of the Conformation and Dynamics of Flexible Molecules and Nanoparticles in Dilute Solution. *J. Chem. Theory Comput.* **2009**, *5*, 2606−2618.
(44) Rodriguez Schmidt, R.; Hernández Cifre, J. G.; García de la Torre, J. Comparison of Brownian Dynamics Algorithms with Hydrodynamic Interactions. *J. Chem. Phys.* **2011**, *135*, 084116.
(45) Geyer, T.; Winter, U. An $O(N^2)$ Approximation for Hydrodynamic Interactions in Brownian Dynamics Simulations. *J. Chem. Phys.* **2009**, *130*, 114905.
(46) Ando, T.; Chow, E.; Saad, Y.; Skolnick, J. Krylov Subspace Methods for Computing Hydrodynamic Interactions in Brownian Dynamics Simulations. *J. Chem. Phys.* **2012**, *137*, 064106.

DOI: 10.1021/acs.jpcb.5b04675
J. Phys. Chem. B 2015, 119, 8425−8439